JET-P(93)104

Alpha Particle Diagnostics using 140GHz Microwave Scattering on JET

J A Hoekzema, A E Costley, T P Hughes, P E Stott.

JET Joint Undertaking, Abingdon, Oxon, OX14 3EA, UK.

Preprint of a paper to be submitted for publication in the Proceedings of the 2nd International Workshop on Strong Microwaves in Plasmas, Moscow, Nizhny Novgorod, Russia, 15-22 August 1993.

December 1993

ABSTRACT

To evaluate the efficiency of alpha particle heating in the DT phase of JET, measurement of the energy distribution of the fast alpha particle population is necessary. The fast ion and alpha particle diagnostic at JET will use collective Thomson scattering of high power microwave radiation to determine the alpha particle velocity distribution between their birth energy (3.5 MeV) and ~0.5 MeV with a typical spatial resolution <0.1 m and time resolution ~0.1 s. The diagnostic uses a high power long pulse 140 GHz gyrotron as the source of probing radiation and a heterodyne receiver system to measure the spectrum of scattered radiation.

1. INTRODUCTION

It is expected that JET will reach plasma parameters near scientific breakeven during the D(euterium)T(ritium) phase. Since the alpha particle heating power will amount to only 20% of the additional heating power, the energy balance will not be dominated by alpha particle heating (except possibly locally) and a detailed analysis of the fast alpha particle behaviour will be necessary to determine the efficiency of alpha particle heating. Fast (i.e. not yet thermalised) alpha particle densities are expected to amount to a few tenths of a percent of the electron density, n_e, at higher values of n_e (~10^{20} m^{-3}) and to a few percent at low n_e where the slowing down is relatively slow. Collective effects, including alpha particle pressure effects can therefore be reactor relevant.

A variety of diagnostics will be used for alpha particle measurements. They include measurement of the source profile (neutron diagnostics), slowed down (ash) and fast alpha particle distributions up to at least 0.5 MeV (charge exchange diagnostics), edge densities (Ion Cyclotron Emission) and escaping alphas. The fast ion and alpha particle diagnostic [1] is aimed at measuring the velocity distribution of alphas between 0.5 and 3.5 MeV and will therefore be especially relevant to study anomalous fast alpha losses (if they occur) which could reduce the efficiency of alpha particle heating.

Use of the diagnostic is not limited to the DT phase of JET. Important fast ion populations are already created by the heating systems and can be measured. The measurement of the thermal ion feature, which dominates the spectrum in a different frequency range can give important information on several plasma

parameters. Also, the power of the probing radiation necessary for alpha particle measurements is sufficient to be used for heat pulse propagation measurements.

2. PRINCIPLE

When a beam of electromagnetic radiation is launched into the plasma, a very small fraction of the power will be scattered from fluctuations in the dielectric properties of the plasma. If the incident beam has wave vector $\mathbf{k}_i$ and frequency ν_i than the scattered radiation detected with wave vector $\mathbf{k}_s$ and frequency ν_s will be due to fluctuations with wave vector $\mathbf{k}$ such that

$$\mathbf{k} = \mathbf{k}_s - \mathbf{k}_i$$

and if $|\mathbf{k}_s|$ and $|\mathbf{k}_i|$ are almost equal,

$$|\mathbf{k}| = 2|\mathbf{k}_i|\sin(\theta/2)$$

where θ is the angle between the incident and scattered directions.

In many experimental situations the main contribution to the scattering comes from electron density fluctuations. In this case the theory is well known. If the wave vector of the fluctuations is small compared to the reciprocal of the Debye length in the scattering volume, the shielding electrons moving with each ion will scatter collectively and the scattered spectrum will be affected by the ion velocity distribution. The components along $\mathbf{k}$ of the ion velocities $\mathbf{v}_i$ of unmagnetised ions are mapped on to the frequency shift of the scattered radiation from the incident beam frequency:

$$\Delta\nu = \nu_s - \nu_i = \mathbf{k}.\mathbf{v}_i/2\pi$$

The thermal ions have relatively low velocity and form a narrow central feature in the scattered spectrum. Alpha particles, slowing down in the plasma from a birth energy of 3.5 MeV, and other fast ions form a distinctive feature which extends to larger frequency shifts. In relativistic, magnetised plasmas such as those in JET, the magnetic field affects the motion of the particles. The dielectric properties of the plasma are important and have been extensively investigated theoretically. In particular for eX(traordinary) to X mode scattering the scattering for frequencies between the fundamental Electron Cyclotron frequency and the R

cutoff is much stronger than for O(rdinary) to O mode scattering [2]. The parameters determining the R cutoff have been discussed by Bindslev ([3,4]), who has given expressions convenient for numerical evaluation. Use of the X mode is however more restricted than the O mode due to the lower density cutoff.

If the scattering wave vector **k** is in a direction nearly perpendicular to **B** strong resonances can occur in the scattering spectrum. Fluctuations in other quantities such as the magnetic field and the electron velocity also become important. In this case a more detailed theoretical treatment is necessary. Extensive calculations are in progress following initial work by Aamodt and Russell [5,6], Chiu [7] and Bindslev [8]. Although the scattered power is much enhanced in these conditions, interpretation of the scattered spectrum in terms of fast ion velocity distributions will be difficult (if at all possible). On the other hand, when the scattering geometry is chosen such that these effects are avoided (i.e. by avoiding **k** close to perpendicular to **B**), mapping of the scattered spectrum to the alpha particle velocity distribution in the region where the alpha feature dominates the spectrum is straightforward [1].

3. PARAMETERS OF THE DIAGNOSTIC SYSTEM

3.1 Frequency

The probing frequency for the diagnostic is 140 GHz and this is the optimum value when JET is operated at full field (3.4 T). This is in the Electron Cyclotron frequency range. Below the fundamental EC frequency the density cut-off severely limits the densities at which measurements can be made (this is less so for a higher field tokamak, e.g. TFTR, where operation at a frequency below the fundamental is of interest) while at frequencies above the EC spectrum no suitable source exists (with possibly an exception for the CO_2 laser frequency which however would necessitate very small scattering angles, ~0.1°, with a consequent loss of spatial resolution). At 140 GHz both the fundamental and second harmonic EC resonance are present in the plasma, located at the very edges. This means that EC emission, against which the scattered radiation has to be discriminated, has a minimum around this frequency. The plasma still acts as an efficient dump for the radiation after reflection(s) off the wall. The plasma is accessible for the radiation if near vertical injection is used up to densities $>2\times10^{20}$ m^{-3} when radiation is coupled to the O(rdinary) mode in the plasma. The alpha-feature dominates part of the spectrum even at large scattering angles (up to at

least 60°) as long as the scattering vector is not near perpendicular to the magnetic field direction, and good spatial resolution for the measurements can be obtained.

3.2 Geometry

The probing radiation will be launched from a top port using a mirror assembly which launches a focused Gaussian beam which reaches a waist radius of 30 mm in the midplane of the torus. A similar Gaussian beam is collected by a receiver mirror assembly in the bottom part of the torus. The scattering volume, determined by the overlap of injected and detected beams is cigar shaped, with a height dependent on the scattering angle. The spatial resolution for the measurement depends on θ but will generally be better than 100 mm.

Both the launch and receive front mirrors are steerable in two independent directions (poloidal and toroidal). In the poloidal direction, mirror rotation by up to ±15° is possible and this is sufficient to scan the scattering volume across the plasma midplane. In the toroidal direction the mirror rotation is limited to ±7.5°. A small angle in the toroidal direction is necessary to allow the choice of a scattering geometry with **k** away from perpendicular to **B**. Changing the angle in the toroidal direction also makes it possible to measure the velocity distribution along different **k** directions to determine the anisotropy (if any) of fast ion populations.

3.3 Polarisation

The polarisation of injected and detected radiation will be chosen such that the radiation is coupled either to the O mode or the X mode in the plasma. In general this will mean elliptic polarisation both for the X and the O mode. For propagation near perpendicular to **B** access is possible up to the density cutoff at $n_e = 2.4\ 10^{20}\ m^{-3}$, although severe refraction effects will complicate measurements when n_e approaches this value. Measurements using the X mode will be limited to $n_e < 6\ 10^{19}\ m^{-3}$ due to the R cutoff and refraction. Accessibility is more restricted for the X mode because the 2nd harmonic resonance is very wide and absorption excludes access to the outboard plasma region.

4. EXPECTED PERFORMANCE

4.1 Overlap of injected and detected beams

At higher densities refraction of the radiation in the plasma can be important. Ray tracing calculations will therefore be done to define the proper antenna orientations on the basis of expected plasma parameters. After the measurement the actual location of the scattering volume can be recalculated using the actual plasma parameters. The injected and detected beams are affected somewhat differently by refraction. This is due to the fact that neither the plasma nor the scattering geometry will be up-down symmetric after the installation of the pumped divertor in JET. As a result, the overlap of the beams may not be optimal if plasma parameters change or are different from expected. In the worst case the beams may even miss each other. At low densities refraction is less important but even here there is some concern that the overlap could be less than optimal due to differential movement of the antenna assemblies. These are mounted on the vessel wall (support independent of the vessel is no longer possible after the divertor installation) which is subject to up to a few cm. movement due to thermal effects and electromagnetic forces.

For these reasons a feedback system is being developed which will adjust the orientation of the steerable receive mirror to obtain optimum overlap. The feedback system will use signals from slave receivers which look in directions slightly displaced from the main beam and with wider antenna patterns (see fig. 2).

There are 4 slave receivers but only 2 will be used at any one time (i.e. an opposite pair). The pair that is used depends on which angle (toroidal or poloidal) of the mirror is best adjusted for the selected scattering geometry. Signals collected by the slave receivers will be integrated over the spectrum, with a band surrounding the gyrotron frequency being filtered out by a notch filter to avoid stray light. Since part of the thermal ion feature is still included, the signals will be relatively strong and short integration times (1 ms) can be used. The feedback response time is however limited by mechanical constraints (mirror inertia) and fast changes in overlap (e.g. as a result of MHD events) can only be slowly corrected (~100 ms).

4.2 Signal to noise

The scattered signal will have to be detected against background EC Emission with measured effective blackbody temperature of several hundred eV [9]. For comparison, the scattered signal will have an effective blackbody temperature of only a few eV in the spectral range dominated by the alpha feature. In order to discriminate between the scattered signal and the background, the injected power will be modulated (generally between maximum and zero power although part modulation is also possible).

Statistical fluctuations on the background radiation will be the main source of noise for the measurement. The signal to noise ratio can be increased by increasing the integration time, using pulse addition techniques. Values of the signal to noise ratio vary with plasma conditions, scattering geometry, mode and frequency. Assuming 5 MW of alpha heating, classical slowing down, no anomalous diffusion, a scattering angle of 20^{o}, background temperature 500 eV, modulation depth of injected power 400 kW, integration time 200 ms and O to O mode scattering with the scattering volume located in the central plasma region, average signal to noise ratios (i.e. averaged over the alpha feature) of 5 (at $n_e=1.5\times10^{20}$ m^{-3}) to 50 (at $n_e=2\times10^{19}$ m^{-3}) have been calculated. Signal to noise values can be increased slightly by reducing the spectral resolution (i.e. by combining detection channels) and dramatically if the X mode can be used.

4.3 Frequency of modulation

Since most of the injected radiation will be absorbed in the plasma after reflection off the vessel wall, this will affect the electron velocity distribution and therefore the ECE [10] which will also show a slight modulation. Although this modulation is mainly out of phase with the scattered radiation, it should be kept fairly small (at most at a level comparable to the scattered radiation). This is possible by choosing a high modulation frequency. Detailed calculations (taking non-thermal effects into account) indicate that a modulation frequency of 10 kHz should be sufficient and this will be the normal choice.

5. TECHNICAL IMPLEMENTATION

The main components of the diagnostic system, shown schematically in fig.3, are a high power gyrotron with associated equipment, RF transmission lines and antennae and a heterodyne detection system.

5.1 Source of probing radiation

A high power, long pulse RF source is necessary for the diagnostic to obtain sufficient signal to noise for alpha particle measurements. The selected gyrotron is capable of operation at up to 300 kW average in long pulses (5 s.). The output of the gyrotron is in the $TE_{15,2}$ mode and this mode is converted to a Gaussian beam external to the gyrotron. The gyrotron has a modulating anode and anode voltage modulation can be used to modulate the RF output power. For full anode modulation (i.e. between -3 kV and ~25 kV relative to the cathode), the electron beam is suppressed during the down phase and for 50% modulation duty cycle the peak RF power can be above 500 kW. The existing Anode Modulator is not capable of full modulation at sufficiently high frequency but can part modulate (i.e. by a few kV) the anode voltage. In this case the electron beam is not suppressed and the peak power has to be reduced. Therefore, a special Anode Modulator is being developed which is capable of full anode voltage modulation at frequencies well above 10 kHz. Power dissipation in this unit is limited by storing the energy, removed from the stray anode capacitance in an external capacitor (gated sinusoidal oscillator) [11].

The gyrotron frequency is stable to within ~100 MHz and the spectral purity is high (noise power outside the main frequency $P_N < 10^{-18} P_o/Hz$, where Po is the total RF power, in the frequency of interest). These properties are necessary to avoid stray light problems:

Some stray radiation will inevitably be collected by the receiver and also radiation scattered by coherent density fluctuations (waves, instabilities) with very small frequency shifts will be at a level many orders of magnitude above the level of radiation scattered on thermal fluctuations. It is estimated that the received radiation with frequency close to the gyrotron frequency will only be 70 dB down on the injected power. This is at a level where it will upset detection (the power in the fast ion feature is ~130 dB down). For this reason frequencies close to the gyrotron frequency are attenuated (~-40 dB) by means of a notch filter. Obviously

the frequency of the gyrotron should be sufficiently stable to stay within the notch bandwidth, which should not be very wide to avoid losing important spectral information. A high spectral purity is necessary because stray radiation at different frequencies cannot be discriminated from scattered radiation at these frequencies.

The gyrotron filament is heated by an AC current. Since the filament current (the associated magnetic field) has some effect on the gyrotron RF output, the frequency of the filament supply will be chosen equal to the anode modulation frequency and phase locked to it, to produce a reproducible RF waveform. The filament current will be boosted for long pulses using an adaptive boost control (i.e. it learns from experience) [11].

A control system to control the parameters of gyrotron operation as well as the scattering parameters (angle of injection, polarisation) and settings of the detection system has been implemented local to the gyrotron area. It is being extended to remote control from the diagnostic control room. A link to the mainframe IBM will make it possible to set up the optimum scattering geometry on the basis of numerical computations (e.g. ray tracing).

The technical systems are protected by a fast protection system which has several levels of intervention, dependent on the fault condition. Intervention ranges from interruption of the pulse for a short time (by rolling back the main Regulator tetrode) to full crowbar of the 100 kV supply voltage. Protection features include protection against operation at the wrong frequency, against operation with a too hot torus window, against excessive power collected by the receiver, against operation without plasma as well as all features standard to a gyrotron system (arcing, reflected power etc.).

5.2 High power transmission

The RF power is transmitted to the torus using a combination of quasi-optical and in-waveguide transmission [12,13].The transmission system is wide band (110-180 GHz) and could therefore be used at other frequencies, which would for instance be of interest if stepped tunability of the gyrotron would be possible. The system is schematically shown in fig. 4.

The $TE_{15,2}$ mode generated by the gyrotron is converted to a Gaussian beam using a quasi-optical mode converter. A high efficiency converter, using deformations of the feed waveguide, is in preparation at Stuttgart University to replace the existing standard converter. The feed waveguide of the converter has an internal diameter of 88.9 mm, equal to the gyrotron output waveguide. This requires large dimensions (the total height of the converter is 4 m.) but avoids a downtaper and consequent reflection of spurious high order modes and should give high power (MW) handling capability at atmospheric pressure. The converter is mounted inside an airtight and radiation tight box (PVC with Al cladding) and stray radiation is mainly absorbed by water in low velocity cooling channels. The required polarisation of the radiation is also produced quasi-optically. The linear polarisation at the output of the mode converter is converted to the required elliptical polarisation by means of a universal polariser. This consists of a rooftop mirror facing a corrugated mirror [12]. Rotation of the polariser as a whole rotates the polarisation while rotation of the corrugated mirror creates the required amount of ellipticity. The polariser is also mounted inside an airtight box. An arc detector, looking at the corrugated mirror, will be incorporated.

After the polariser, the radiation is coupled at the beam waist into 88.9 mm ID corrugated waveguide, using the excellent coupling of a Gaussian beam to the $HE_{1,1}$ mode. The waveguide run is 60 m. long and includes 7 mitre bends. The relatively large diameter of the waveguide will allow high power transmission at atmospheric pressure. In fact the whole transmission system will be at a slight under pressure, equal to the pressure inside the torus hall. Precise alignment of the waveguide (radius of curvature > 3 km) is crucial to avoid mode conversion. Alignment is achieved by precise machining of the 2 m. long waveguide sections and supporting them by constant spring supports which are adjusted individually to counterbalance the weight of the sections. Alignment is then determined by the quality of machining of waveguide and flange connections and the waveguide can move to eliminate the effect of moving support structures (e.g. due to thermal effects). Expansion joints are included and allow fixed positions of the waveguide at both ends and at the torus hall penetration. Most of the waveguide is made of electroformed copper with NiP coating but more resistive sections (plasma sprayed stainless steel) are included after each bend. The increased resistivity has negligible effect on transmission of the $HE_{1,1}$ mode, but attenuates any high order modes created at the bends. Forward and reflected power measurements are done by coupling some radiation through an array of small (cut-off) holes in one of the mitre bends. By switching a mitre bend the

radiation can be re-routed to a silicon oil cooled calorimeter. A mechanical shutter is included in the line for safety reasons.

Near the torus the transmission switches back to quasi-optical transmission. The Gaussian beam, launched from the waveguide is allowed to expand to reduce the power density at the torus window. Two slightly ellipsoidal parallel mirrors mounted on the vessel at the top of the port correct for differential movement between the end of the waveguide and the vessel (the vessel moves up and out due to thermal expansion and atmospheric and magnetic pressures). A focused beam is launched down the port which reaches a waist radius of 27.8 mm in the port (optimum waist to avoid beam truncation in the narrow port).

5.3 Torus windows

The gyrotron window is a double disk sapphire window with fluorocarbon face cooling between the disks. This type of window is not suitable as a torus window because the transmission capability is much less for a Gaussian beam than it is for the $TE_{15,2}$ mode, because safety margins for JET torus windows are larger than for gyrotron windows and because of the risk of fluorocarbon contamination of the vacuum vessel. The high power torus window is an inertially cooled waterfree fused silica disk with 190 mm clear view. This material has been selected because of the low loss, low expansion, relatively low refractive index and limited temperature dependence of this index [14]. In view of the large beam radius at the window (45.5 mm) the temperature rise during a pulse should be tolerable. The main drawback of this material is the low thermal conductivity which will limit the duty cycle. By allowing the start of a new pulse before the window is completely cooled down (but still at a temperature of a few hundred ^{o}C in the centre), radiative cooling should be sufficient in between JET pulses. The window is resonant at 140 GHz, 200 ^{o}C to avoid reflection as much as possible and the thickness is chosen at 10 wavelengths. This thickness would be suitable for stepped tuning of the gyrotron to neighbouring $TE_{n,2}$ modes (the window would still be resonant to good approximation).

The high power window will be replaced (like all JET windows) by a double disk window assembly before the DT phase (1996). For this window assembly several options are being considered, including a double disk sapphire window with cryogenic (liq. N_2) edge cooling.

On the receiver side, double disk crystal quartz windows, already suitable for the DT phase, will be installed. Over a wide bandwidth these window assemblies show wild variations of transmission efficiency (between 20 and 100%) as a function of frequency. Although some loss of signal could be tolerated, since also the main source of noise would be attenuated (ECE), calibration would be difficult especially if thermal effects would be important. Fortunately the required bandwidth of the scattered signals is restricted. The bandwidth of the slave signals is < 1 GHz in which case it is sufficient to choose a resonant thickness for both disks to obtain almost full transmission. For the main scattered signal a reasonable behaviour of the transmission over the bandwidth of 134 to 146 GHz can be obtained by also controlling the distance between the disks precisely at a few half wavelengths [15], as illustrated in fig.5.

5.4 In-vessel components

The launch mirror assembly consists of a defocusing hyperboloidal fixed mirror and an ellipsoidal steerable mirror. The required orientation of the last mirror will be set up from a rest position (to which the mirror tends to return due to springs which are incorporated in the assembly) by means of pull rods. The start of movement (in poloidal and toroidal direction) from the rest position is detected by switches. The pull rods are controlled by stepper motors at the top of the port.

Scattered radiation is collected by a receive antenna, consisting of two mirrors; a flat mirror which can be rotated in two independent directions and a fixed ellipsoidal mirror. Mirror movement is again effected by pull rods, which in this case are controlled by more powerful servo motors to minimise feedback response times. The curved mirror focuses a Gaussian beam (with 30 mm waist radius in the centre of the torus) into a 10 mm ID corrugated waveguide. This small diameter is chosen to allow bending the waveguide around the divertor structures in the torus. Four additional corrugated "slave" waveguides, with ID 7.5 mm are bundled with the main receive waveguide. They view the plasma through the same mirror assembly. The waveguide bundle is supported by an inconel structure which is sufficiently flexible to allow the movement of the antenna end of the waveguides, mounted on the torus wall, with the torus while at the other end the waveguides are supported on the transformer limbs. The main receive waveguide is tapered up to 31.75 mm, before going through a mitre

bend and the double disk crystal quartz window. The radiation from the slave waveguides leaves the vacuum quasi-optically.

Relative alignment of the launch and receive mirrors is possible by injecting low power radiation (which is coupled into the high power waveguide) and finding the angles for which the received signal is maximum. This determines the orientation where launch and receive are oriented such that they directly view each other.

5.5 Low power transmission

The main corrugated waveguide is continued to the detection area (40 m.) where the radiation is launched into a quasi optical polariser [16] to select the correct mode ($HE_{1,1}$) and polarisation. The polariser uses two mirrors with rotatable wire grids which act as quarter and half wave plates and can select the desired elliptical polarisation. The slave waveguides end before the vacuum windows and radiation is transmitted through the windows quasi-optically. Outside the vacuum the 2 signals to be used for feedback will be selected. Polarisers (again using mirrors with wire grids) will select the required polarisation and coupling into fundamental waveguide by means of corrugated horn antennas will select the correct mode. After a converter-taper the radiation from two of the slave antennas is transmitted to the slave detection systems in the $TE_{1,1}$ mode in 27.8 mm smooth waveguide.

5.6 Detection

The super heterodyne detection system [17] measures the spectrum of scattered radiation between 134 and 146 GHz in 32 spectral channels. The bandwidths of the different channels are chosen to be proportional to their displacement from the central frequency (see fig 1). Fig 7 gives a schematic of the system. The 134-146 GHz spectral region is downconverted to 6-18 GHz. In order to correct for frequency drift of the gyrotron or local oscillator, which is important for the central portion of the frequency region, this part is downconverted again using a local oscillator which is derived from the frequency difference between first LO and gyrotron. The frequency discrimination is performed by 32 bandpass filters and the signals are detected by Schottky detectors.

To recover the scattered signal from the background a data acquisition system has been built to sample the scattered signal at up to 5 megasamples/s and perform coherent addition of the signal in real time. In standard operation it is expected that 10 or more pulses will be added (during 1 ms) to give a single pulse form, characterised by 20 points. Further pulse addition will then be done in hardware.

6. STATUS

During the last JET operational period the receiver system was used for passive measurements of the background radiation. These measurements confirmed expectations with respect to the background radiation level, which is important since statistical fluctuations on the background radiation are the main source of noise for the measurement. Transmission systems have been tested at low power, at which they perform satisfactorily. Presently, a prototype gyrotron, on loan from the US DoE, is being commissioned, while a commercial gyrotron is now scheduled for delivery in early '94. New in-vessel components are being installed to make the diagnostic compatible with the new divertor geometry of JET. First plasma measurements are expected to be done after JET operation is resumed in '94 and will concentrate on measurements of the thermal ion feature and on fast ions created by the heating systems (mainly ICRH).

ACKNOWLEDGEMENT

There is a formal collaboration with the US DoE on this diagnostic, involving equipment and personnel from MIT and LLNL.

REFERENCES

[1] Costley AE et al, JET Report, JET-R(88)08,1988
[2] Hughes TP and Smith SRP, J. Plasma Phys. **42**,215 (1989)
[3] Bindslev H, Plasma Phys. and Contr. Fusion **33**,1775 (1991)
[4] Bindslev H, Plasma Phys. and Contr. Fusion (in press) (1993)
[5] Aamodt RE et al, Rev. Sci. Instr. **61**,3211 (1990)
[6] Aamodt RE et al, Nuclear Fusion **32**,745 (1992)
[7] Chiu SC, Phys. Fluids **B3**, 1374 (1991)
[8] Bindslev H, Plasma Phys. and Contr. Fusion (in press) (1993)
[9] Machuzak JS et al, Rev. Sci. Instr. **63**,4648 (1992)

[10] Costley AE et al, Proc. 7th Int. Workshop on ECE and ECRH (EC7), Hefei (1989)
[11] Hoekzema JA et al, 16th Symp. on Fusion Technology, London, JET Report JET P(90)56 Vol 1, 61 (1990)
[12] Thumm M et al, Report IPF Stuttgart (1988)
[13] Hoekzema JA et al, 15th Symp. on Fusion Technology, Utrecht, Vol 1,314 (1988)
[14] Birch JR et al, 18th Int. Conf. on IR an mm waves, Un. of Essex, Sept. 1993
[15] Hughes TP et al, 18th Int. Conf. on IR an mm waves, Un. of Essex, Sept. 1993
[16] Harvey AR, Int J. IR and mm Waves, Vol 14, no 1 (1993)
[17] Fessey JA et al, 18th Int. Conf. on IR an mm waves, Un. of Essex, Sept. 1993

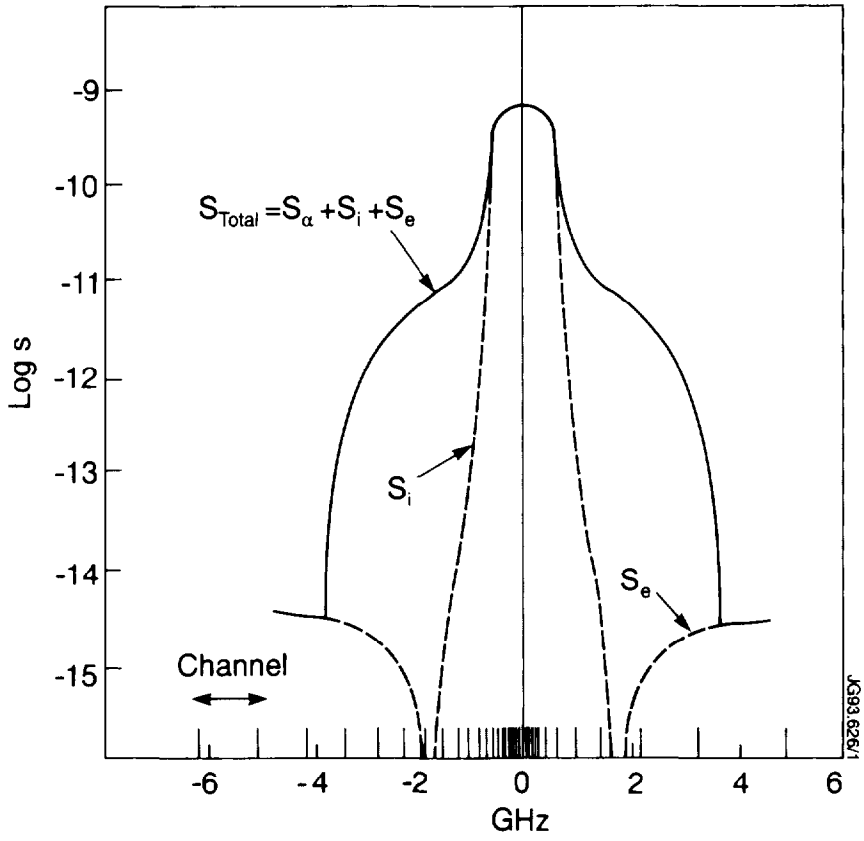

Fig 1: Typical calculated spectrum of scattered radiation showing the contributions of thermal ions, alpha particles and electrons to the spectrum. In part of the spectral region, corresponding to alpha energies between ~0.5 and 3.5 MeV the alpha feature dominates the scattered spectrum.

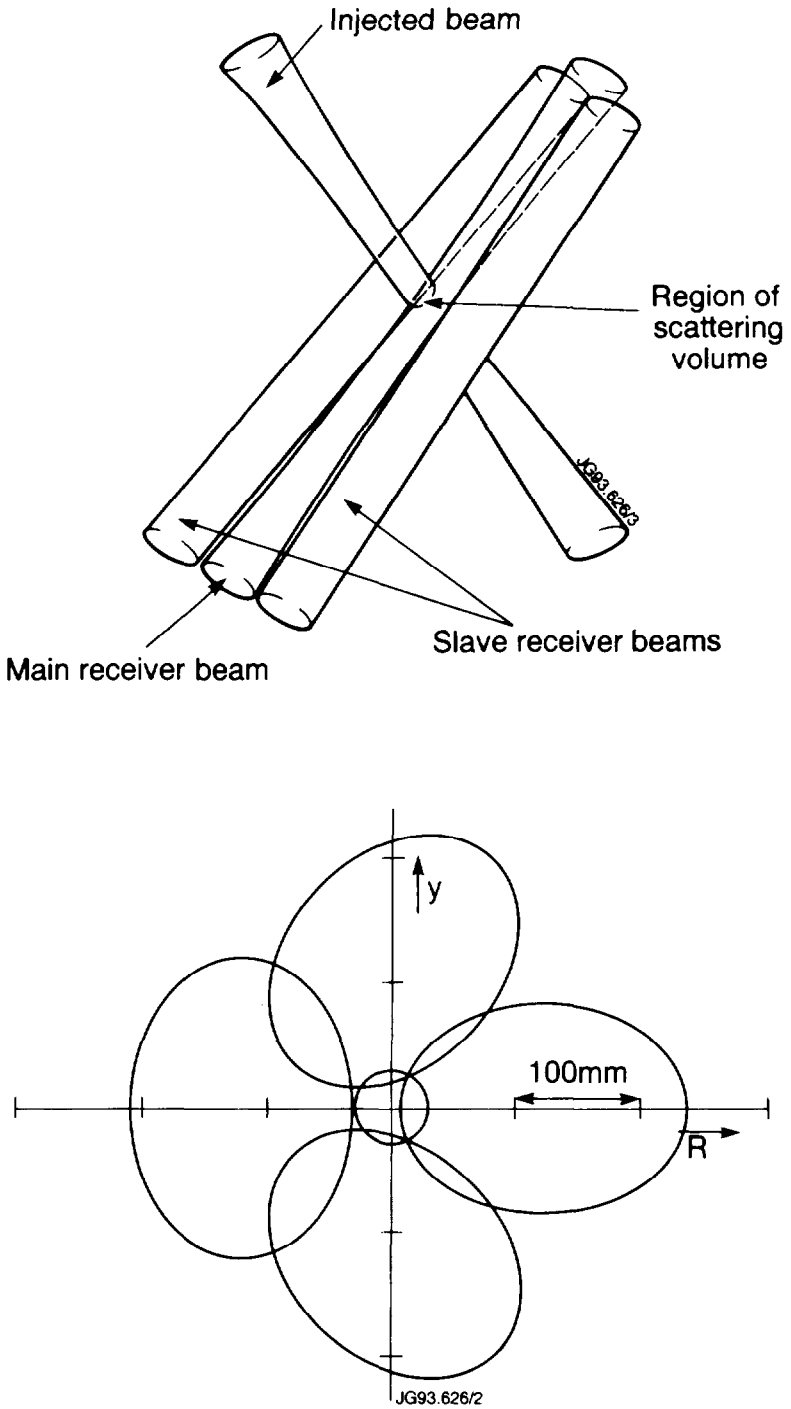

Fig 2: Schematic view of the scattering volume with two "slave" beams and the intersection of the main beam and surrounding slave beams with the torus midplane (1/e intensity contours).

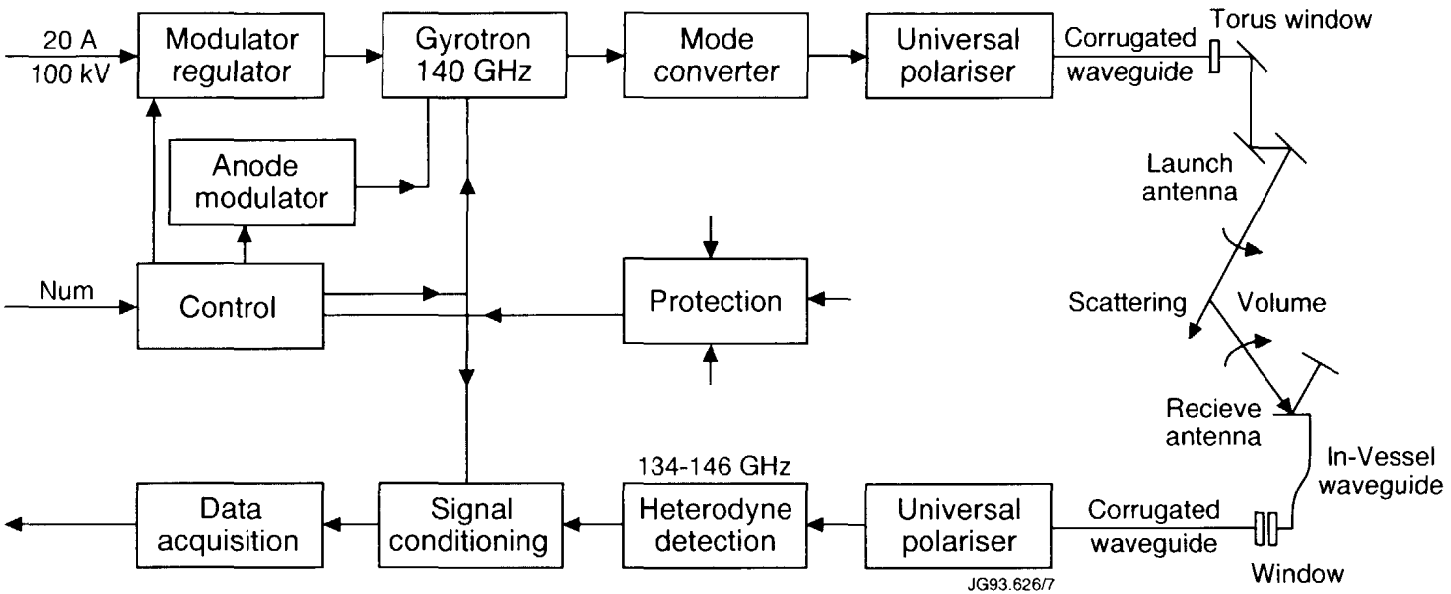

Fig 3: Schematic overview of the diagnostic system

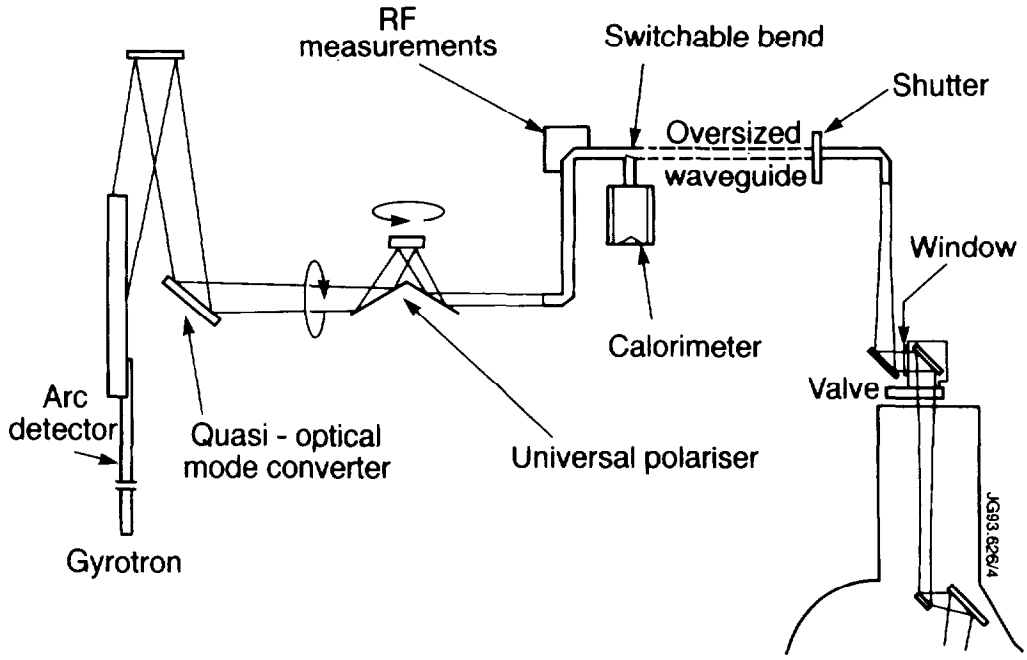

Fig 4: The high power transmission system

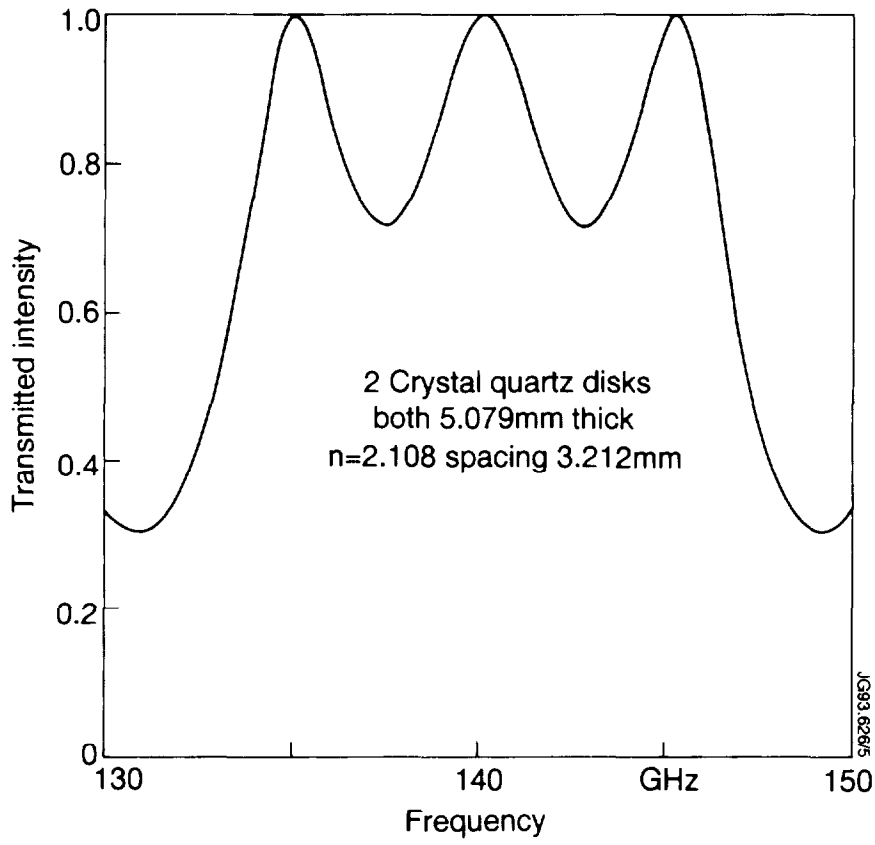

Fig 5: Transmission efficiency between 134 and 146 GHz of a double disk crystal quartz window (optimum interspace).

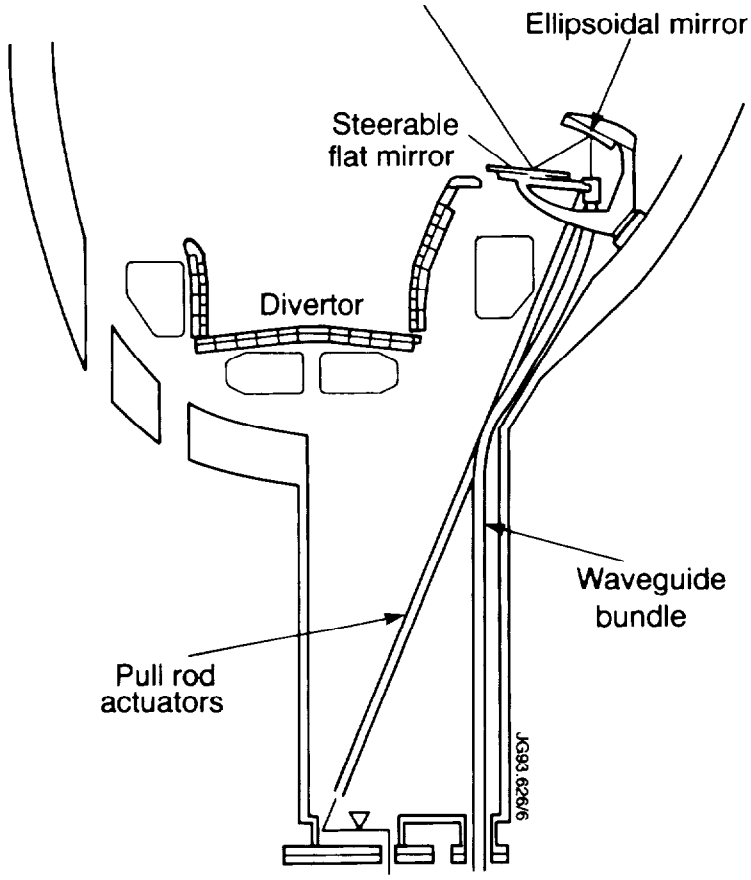

Fig 6: Receiver antenna assembly and waveguide bundle, containing a main and 4 slave corrugated waveguides, in the bottom part of the vessel.

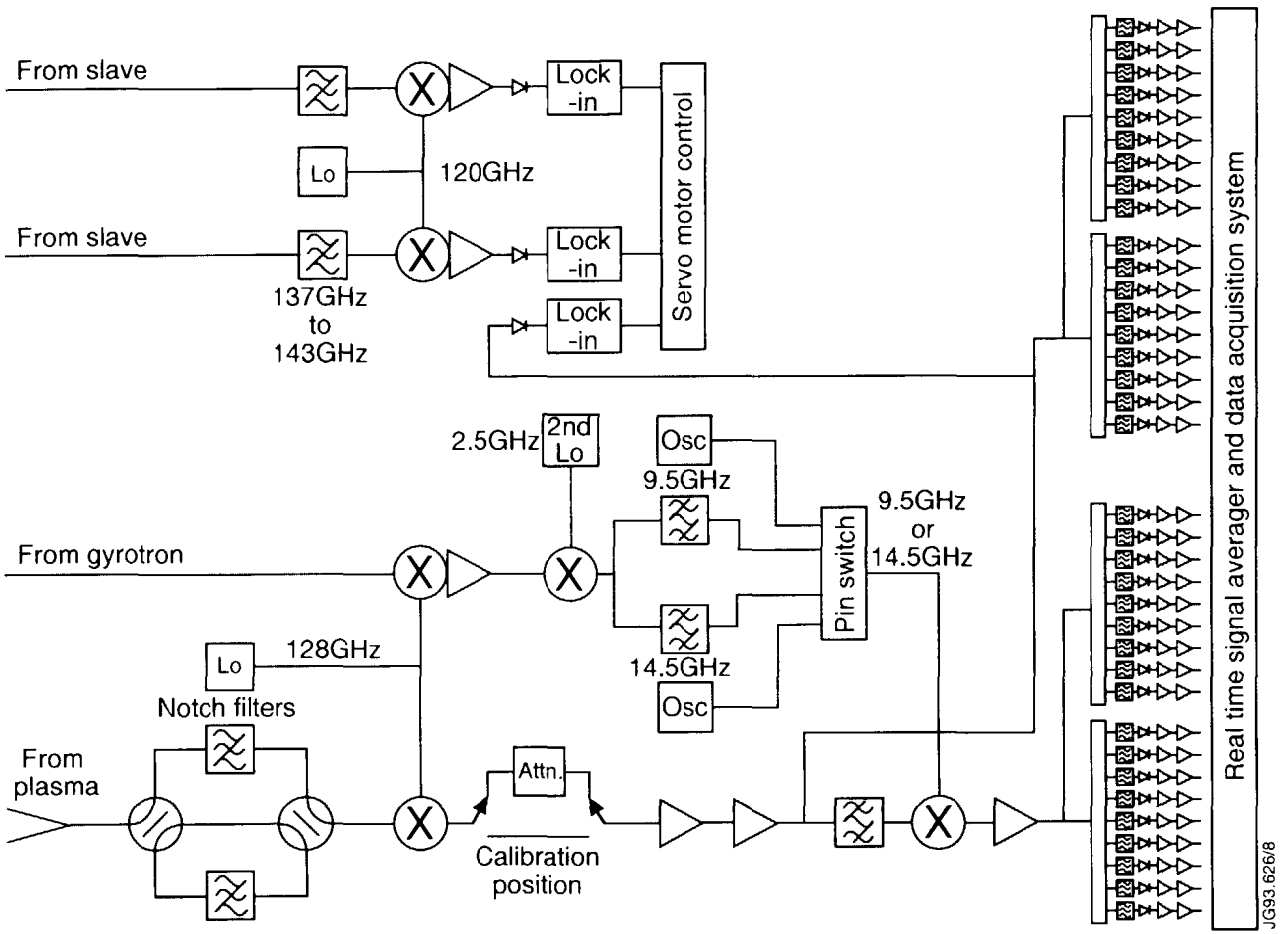

Fig 7: Schematic of the detection system